Check for updates

Low-energy Ga₂O₃ polymorphs with low electron effective masses†

Qingyang Fan, [ID] *[ab] Ruida Zhao,[a] Wei Zhang, [ID] [c] Yanxing Song,[c] Minglei Sun [ID] [d] and Udo Schwingenschlögl [ID] *[d]

We predict three Ga₂O₃ polymorphs with $P2_1/c$ or $Pnma$ symmetry. The formation energies of $P2_1/c$ Ga₂O₃, $Pnma$-I Ga₂O₃, and $Pnma$-II Ga₂O₃ are 57 meV per atom, 51 meV per atom, and 23 meV per atom higher than that of β-Ga₂O₃, respectively. All the polymorphs are shown to be dynamically and mechanically stable. $P2_1/c$ Ga₂O₃ is a quasi-direct wide band gap semiconductor (3.83 eV), while $Pnma$-I Ga₂O₃ and $Pnma$-II Ga₂O₃ are direct wide band gap semiconductors (3.60 eV and 3.70 eV, respectively). Simulated X-ray diffraction patterns are provided for experimental confirmation of the predicted structures. The polymorphs turn out to provide low electron effective masses, which is of great benefit to high-power electronic devices.

Introduction

Wide band gap semiconductors are important for devices requiring high frequency, temperature, and/or power.[1] Many commercial applications use the third generation semiconductors GaN and SiC. However, those suffer from high manufacturing costs and limitations of the achievable performance.[2,3]

Gallium oxide, especially thermodynamically stable β-Ga₂O₃, attracts more and more attention, because its high breakdown field leads to a higher Baliga figure of merit for application in high-power electronic devices than provided by SiC and GaN.[4] The most famous polymorphs of Ga₂O₃ are the α-, β-, γ-, δ-, and ε-phases,[5,6] which are similar in properties such as the band gap, elastic modulus, and electron effective mass.[7] The hexagonal structure of ε-Ga₂O₃ with space group $P6_3mc$ enables heteroepitaxial growth on GaN, AlN, ZnO, and Al₂O₃.[8] While theoretical studies focus on the orthorhombic $Pna2_1$ phase,[7,9–12] experiments show that ε-Ga₂O₃ is pyroelectric with large polarization and piezoelectric coupling, being able to host a high density electron gas. Various theoretical studies address the physical properties of the β-phase and experimental studies the preparation of non-β-phases.[12–25]

[a] *College of Information and Control Engineering, Xi'an University of Architecture and Technology, Xi'an 710055, China*

[b] *Shaanxi Key Laboratory of Nano Materials and Technology, Xi'an, 710055, China. E-mail: fanqy@xauat.edu.cn*

[c] *School of Microelectronics, Xidian University, Xi'an 710071, China*

[d] *Applied Physics Program, Physical Science and Engineering Division, King Abdullah University of Science and Technology (KAUST), Thuwal 23955-6900, Saudi Arabia. E-mail: udo.schwingenschlogl@kaust.edu.sa*

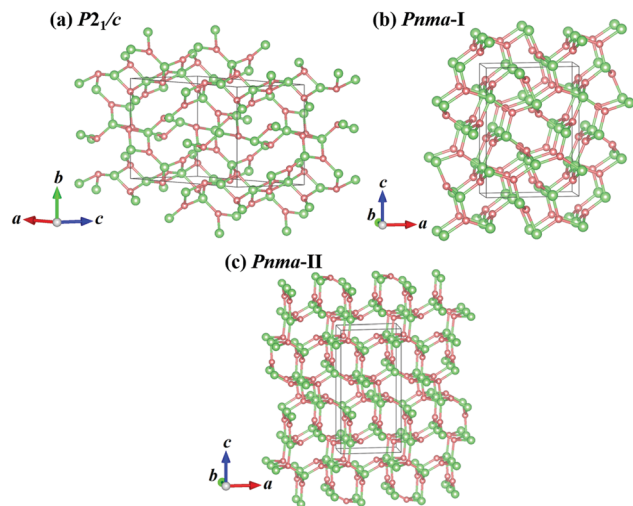† Electronic supplementary information (ESI) available. See DOI: 10.1039/d1cp05271c

In the present work, we predict three Ga₂O₃ polymorphs, which we call $P2_1/c$ Ga₂O₃, $Pnma$-I Ga₂O₃, and $Pnma$-II Ga₂O₃ according to their space groups. The formation energy of $Pnma$-II Ga₂O₃ is found to be 3 meV per atom lower than that of α-Ga₂O₃. A systematic investigation of the predicted polymorphs is performed, including the stability, electronic states, and carrier effective mass.

Computational details

Based on density functional theory, all calculations are performed with the Cambridge Serial Total Energy Package.[26] We use the generalized gradient approximation of Perdew–Burke–Ernzerhof for structure optimization and the Heyd–Scuseria–Ernzerhof hybrid functional for calculating electronic properties. Ultrasoft pseudopotentials[27] and the Broyden–Fletcher–Goldfarb–Shanno scheme are adopted. Brillouin zone integrations are performed on Monkhorst–Pack $8 \times 5 \times 14$, $6 \times 12 \times 4$, and $7 \times 13 \times 3$ k-grids for $P2_1/c$ Ga₂O₃, $Pnma$-I Ga₂O₃, and $Pnma$-II Ga₂O₃, respectively. Elastic constants are calculated by the strain-stress method. Phonon spectra are obtained by density functional perturbation theory.[28]

Results and discussion

The crystal structures of the predicted Ga₂O₃ polymorphs are shown in Fig. 1. In each case the unit cell contains 8 Ga and 12 O atoms. In $P2_1/c$ Ga₂O₃ and $Pnma$-I Ga₂O₃ the Ga atoms are 4- or 5-coordinated and the O atoms are 3-coordinated, whereas in $Pnma$-II Ga₂O₃ the Ga atoms are 4- or 6-coordinated and the O atoms are 3-coordinated (α-Ga₂O₃: O atoms 4-coordinated

This journal is © the Owner Societies 2022

Phys. Chem. Chem. Phys., 2022, **24**, 7045–7049 | 7045

Fig. 1 Crystal structures. Red spheres represent O atoms and green spheres represent Ga atoms.

Fig. 2 (a–c) Phonon spectra. (d) Formation energies with respect to β-Ga₂O₃.

and Ga atoms 6-coordinated; β-Ga$_2$O$_3$: O atoms 3- or 4-coordinated and Ga atoms 4- or 6-coordinated). The lattice parameters of the predicted polymorphs are compared to those of α-Ga$_2$O$_3$ and β-Ga$_2$O$_3$ in Table 1. The theoretical values of α-Ga$_2$O$_3$ and β-Ga$_2$O$_3$ show excellent agreement with the experiment (deviation less than 1.8%), demonstrating reliability of the employed theoretical methodology. The densities of the predicted polymorphs are smaller than those of α-Ga$_2$O$_3$ and β-Ga$_2$O$_3$.

The phonon spectra of the predicted polymorphs are shown in Fig. 2. Absence of imaginary frequencies indicates dynamical stability. Fig. 2(d) gives the formation energies of selected polymorphs with respect to that of β-Ga$_2$O$_3$ (minimum). The values of the predicted polymorphs are much lower than those of polymorphs from the Materials Project (mp). We calculate for mp-13134 a value of 280 meV per atom in agreement with the mp-result of 284 meV per atom. The formation energies of $P2_1/c$ Ga$_2$O$_3$, $Pnma$-I Ga$_2$O$_3$, and $Pnma$-II Ga$_2$O$_3$ are only moderately higher (57 meV per atom, 51 meV per atom, and 23 meV per atom, respectively) than that of β-Ga$_2$O$_3$. The formation energy of $Pnma$-II Ga$_2$O$_3$ is even 3 meV per atom lower than that of α-Ga$_2$O$_3$. To verify the stability of the predicted polymorphs at operating temperature, *ab initio* molecular dynamics simulations are performed at 1000 K (5 ps with a time step of 1 fs). The results in Fig. 3 show no indication of structural instability.

The elastic matrix of monoclinic $P2_1/c$ Ga$_2$O$_3$ has 13 independent constants and the elastic matrices of orthorhombic
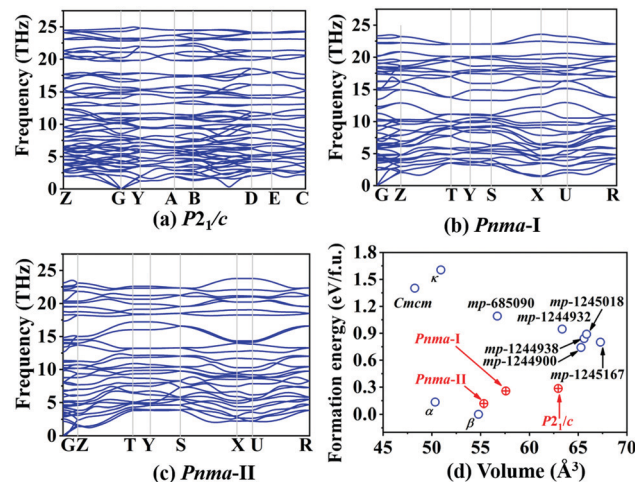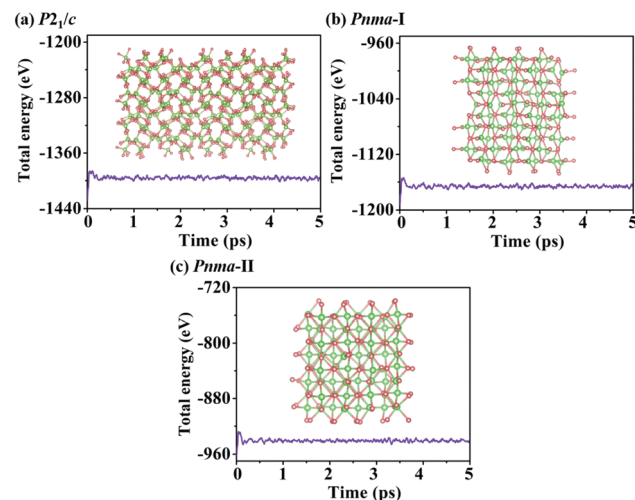

Fig. 3 *Ab initio* molecular dynamics simulations at 1000 K: total energy and final structures.

$Pnma$-I and $Pnma$-II Ga$_2$O$_3$ have 9 independent constants. The obtained elastic matrices and the Born mechanical stability conditions are given in the ESI† material. The elastic constants in Table 2 show that the Born mechanical stability criteria are fulfilled for all the predicted polymorphs. The bulk modulus B, shear modulus G, and Young's modulus E of $Pnma$-II Ga$_2$O$_3$ are found to resemble the values of β-Ga$_2$O$_3$ (Table 2).

The obtained electronic band structures in Fig. 4 show a quasi-direct band gap for $P2_1/c$ Ga$_2$O$_3$ (3.83 eV) and direct band

Table 1 Lattice parameters and densities

Ga₂O₃		a (Å)	b (Å)	c (Å)	β (°)	ρ (g cm^{-3})
α	Theory	4.988		13.625		6.46
	Exp.[29]	4.983		13.433		6.47
β	Theory	12.452	3.083	5.876	103.7	5.68
	Exp.[30]	12.230	3.040	5.800	103.7	5.94
$P2_1/c$	Theory	9.770	8.762	5.810	149.6	4.95
$Pnma$-I	Theory	7.073	3.311	9.835		5.41
$Pnma$-II	Theory	5.900	3.093	12.126		5.63

Table 2 Elastic constants (GPa) and moduli (GPa)

Ga₂O₃	C_{11}	C_{22}	C_{33}	C_{44}	C_{55}	C_{66}	C_{12}	C_{13}	C_{23}	B	G	E
α	365	365	327	75	75	108	149	106	106	197	96	248
β	199	312	298	39	77	95	112	125	62	155	69	180
$P2_1/c$	175	253	204	45	59	47	62	66	88	116	53	138
$Pnma$-I	210	269	257	53	73	51	90	109	122	152	62	164
$Pnma$-II	311	300	193	81	96	41	59	116	120	154	71	185

7046 | *Phys. Chem. Chem. Phys.*, 2022, **24**, 7045–7049

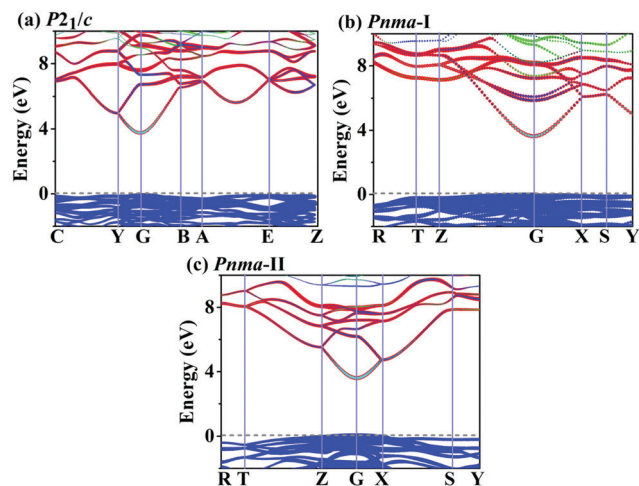This journal is © the Owner Societies 2022

Fig. 4 Electronic band structures. Red, green, cyan, and blue colors represent Ga s, Ga p, O s, and O p contributions, respectively. The high symmetry points are C (0.0, 0.5, 0.5), Y (0.0, 0.5, 0.0), G (0.0, 0.0, 0.0), B (0.5, 0.0, 0.0), A (0.5, 0.5, 0.0), E (0.5, 0.5, 0.5), and Z (0.0, 0.0, 0.5) for $P2_1/c$ symmetry and R (−0.5, 0.5, 0.5), T (−0.5, 0.0, 0.5), Z (0.0, 0.0, 0.5), G (0.0, 0.0, 0.0), X (0.0, 0.5, 0.0), S (−0.5, 0.5, 0.0), and Y (−0.5, 0.0, 0.0) for $Pnma$ symmetry.

Fig. 5 X-Ray diffraction patterns (Cu source with a wavelength of 1.5406 Å).

gaps for $Pnma$-I Ga_2O_3 (3.60 eV) and $Pnma$-II Ga_2O_3 (3.70 eV). Although these band gaps are smaller than that of β-Ga_2O_3 (4.60 eV),[31] they exceed those of SiC (2.40 eV), GaN (3.20 eV), and ZnO (3.44 eV).[32] Note that the calculated band gap of β-Ga_2O_3 is 4.60 eV, in perfect agreement with the experimental result of ref. 31.

We present the calculated electron and hole effective masses along the a-, b-, and c-axes in Table 3. The electron effective masses of $Pnma$-I Ga_2O_3 are similar to those of α-Ga_2O_3 and β-Ga_2O_3, those of $P2_1/c$ Ga_2O_3 are a bit larger, and those of $Pnma$-II Ga_2O_3 are significantly larger by a factor of almost 2.5. We find hardly any anisotropy for the electron effective masses. For $P2_1/c$ Ga_2O_3 the minimum appears not in a special direction, for $Pnma$-I Ga_2O_3 it appears along the a-axis, and for $Pnma$-II Ga_2O_3 it appears along the b-axis. The hole effective masses show significant anisotropy. For both $P2_1/c$ Ga_2O_3 and
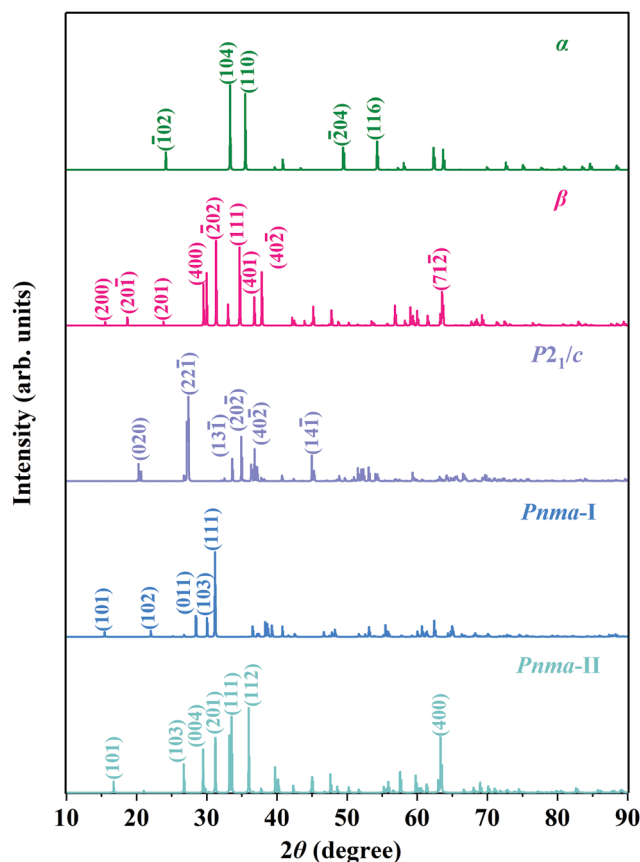
$Pnma$-II Ga_2O_3 the minimum appears along the b-axis and for $Pnma$-I Ga_2O_3 it appears along the c-axis. $P2_1/c$ Ga_2O_3 and $Pnma$-II Ga_2O_3 show heavy fermion behavior in specific directions (Table 3).

The simulated X-ray diffraction patterns of α-Ga_2O_3, β-Ga_2O_3, $P2_1/c$ Ga_2O_3, $Pnma$-I Ga_2O_3, and $Pnma$-II Ga_2O_3 are displayed in Fig. 5. The (111) and (400) peaks of β-Ga_2O_3 (at 34.7° and 29.5°, respectively) coincide with the mp-results. Though they belong to the same space group, the spectra of $Pnma$-I Ga_2O_3 and $Pnma$-II

Table 3 Electron and hole effective masses (multiples of the free electron mass)

| Ga_2O_3 | Electron effective mass | | | | | | |
	m_a	m_b	m_c	m_{max}	Direction	m_{min}	Direction
α	0.21	0.21	0.21	0.21	[1, 1, 1]	0.21	[1, 1, 1]
β	0.22	0.22	0.21	0.23	[0.68, −0.73, 0.02]	0.21	[−0.22, −0.22, 0.95]
$P2_1/c$	0.26	0.26	0.26	0.26	[0, 1, 0]	0.26	[−0.62, 0, 0.78]
$Pnma$-I	0.20	0.23	0.23	0.23	[0, 1, 0]	0.20	[1, 0, 0]
$Pnma$-II	0.51	0.51	0.54	0.54	[0, 0, 1]	0.51	[0, 1, 0]

| Ga_2O_3 | Hole effective mass | | | | | | |
	m_a	m_b	m_c	m_{max}	Direction	m_{min}	Direction
α	2.54	2.54	0.80	3.47	[0.67, 0.67, 0.31]	0.71	[0.25, 0.25, 0.93]
β	2.81	3.49	4.54	6.06	[0.25, 0.56, 0.79]	2.57	[−0.85, −0.53, 0.04]
$P2_1/c$	2.55	2.26	5.03	>50	[−0.56, 0, 0.83]	2.26	[0, 1, 0]
$Pnma$-I	2.29	2.29	0.31	2.29	[1, 0, 0]	0.31	[0, 0, 1]
$Pnma$-II	4.07	0.37	>50	>50	[0, 0, 1]	4.07	[0, 1, 0]

This journal is © the Owner Societies 2022

Phys. Chem. Chem. Phys., 2022, **24**, 7045–7049 | **7047**

Ga$_2$O$_3$ reveal notable differences. The strongest peaks are (22–1) at 27.3° for $P2_1/c$ Ga$_2$O$_3$, (111) at 33.5° for $Pnma$-I Ga$_2$O$_3$, and (112) at 35.9° for $Pnma$-II Ga$_2$O$_3$. The X-ray characteristics enable identification of the predicted polymorphs in future experiments.

Conclusions

In conclusion, three low-energy Ga$_2$O$_3$ polymorphs with wide band gaps are predicted to be dynamically and mechanically stable. $P2_1/c$ Ga$_2$O$_3$ and $Pnma$-I Ga$_2$O$_3$ realize a novel 5-coordination of the Ga atoms. The band gap is quasi-direct for $P2_1/c$ Ga$_2$O$_3$ and direct for $Pnma$-I Ga$_2$O$_3$ and $Pnma$-II Ga$_2$O$_3$. The electron and hole effective masses show significant differences from those of α-Ga$_2$O$_3$ and β-Ga$_2$O$_3$. Simulated X-ray diffraction patterns enable experimental confirmation of the predicted structures. Remarkably, chemical vapor deposition can be used to synthesize a large variety of Ga$_2$O$_3$ polymorphs, adopting temperatures of 410 °C,[33] 550 °C,[34] and 650 °C.[35] When aiming for synthesis of the predicted polymorphs by this method, identifying a suitable growth temperature is the main experimental uncertainty. However, since structural stability is maintained beyond 1000 K, it is reasonable to expect that appropriate growth parameters can be established.

Data availability statement

The data that supports the findings of this study are available within the article and its supplementary material.

Conflicts of interest

The authors have no conflicts to disclose.

Acknowledgements

References

1 C. G. Van de Walle, *Wide-band-gap semiconductors*, Elsevier, Amsterdam, 2012.

2 W. Kowbel, C. A. Bruce, K. L. Tsou, K. Patel, J. C. Withers and G. E. Youngblood, High thermal conductivity SiC/SiC composites for fusion applications, *J. Nucl. Mater.*, 2000, **283–287**, 570–573.

3 J. Kim, D. Tahara, Y. Miura and B. G. Kim, First-principle calculations of electronic structures and polar properties of (κ,ε)-Ga$_2$O$_3$, *Appl. Phys. Express*, 2018, **11**, 061101.

4 M. Higashiwaki, K. Sasaki, H. Murakami, Y. Kumagai, A. Koukitu, A. Kuramata, T. Masui and S. Yamakoshi, Recent progress in Ga$_2$O$_3$ power devices, *Semicond. Sci. Technol.*, 2016, **31**, 034001.

5 R. Roy, V. G. Hill and E. F. Osborn, Polymorphism of Ga$_2$O$_3$ and the system Ga$_2$O$_3$–H$_2$O, *J. Am. Chem. Soc.*, 1952, **74**, 719–722.

6 J. Furthmüller and F. Bechstedt, Quasiparticle bands and spectra of Ga$_2$O$_3$ polymorphs, *Phys. Rev. B*, 2016, **93**, 115204.

7 S. Yoshioka, H. Hayashi, A. Kuwabara, F. Oba, K. Matsunaga and I. Tanaka, Structures and energetics of Ga$_2$O$_3$ polymorphs, *J. Phys.: Condens. Matter*, 2007, **19**, 346211.

8 H. Y. Playford, A. C. Hannon, E. R. Barney and R. I. Walton, Structures of uncharacterised polymorphs of gallium oxide from total neutron diffraction, *Chem. – Eur. J.*, 2013, **19**, 2803–2813.

9 I. Cora, F. Mezzadri, F. Boschi, M. Bosi, M. Čaplovicová, G. Calestani, I. Dodony, B. Pecz and R. Fornari, The real structure of ε-Ga$_2$O$_3$ and its relation to κ-phase, *CrystEngComm*, 2017, **19**, 1509–1516.

10 M. B. Maccioni and V. Fiorentini, Phase diagram and polarization of stable phases of (Ga$_{1−x}$In$_x$)$_2$O$_3$, *Appl. Phys. Express*, 2016, **9**, 041102.

11 M. Kracht, A. Karg, J. Schörmann, M. Weinhold, D. Zink, F. Michel, M. Rohnke, M. Schowalter, B. Gerken, A. Rosenauer, P. J. Klar, J. Janek and M. Eickhoff, Tin-assisted synthesis of ε-Ga$_2$O$_3$ by molecular beam epitaxy, *Phys. Rev. Appl.*, 2017, **8**, 054002.

12 K. Yamaguchi, First principles study on electronic structure of β-Ga$_2$O$_3$, *Solid State Commun.*, 2004, **131**, 739–744.

13 S. Ohira, N. Suzuki, N. Arai, M. Tanaka, T. Sugawara, K. Nakajima and T. Shishido, Characterization of transparent and conducting Sn-doped β-Ga$_2$O$_3$ single crystal after annealing, *Thin Solid Films*, 2008, **516**, 5763–5767.

14 G. Q. Pei, C. T. Xia, Y. J. Dong, B. Wu, T. Wang and J. Xu, Studies of magnetic interactions in Mn-doped β-Ga$_2$O$_3$ from first-principles calculations, *Scr. Mater.*, 2008, **58**, 943–946.

15 W. Z. Xiao, L. L. Wang, L. Xu, Q. Wan and B. S. Zou, Electronic structure and magnetic interactions in Ni-doped β-Ga$_2$O$_3$ from first-principles calculations, *Scr. Mater.*, 2009, **61**, 477–480.

16 Y. J. Zhang, J. L. Yan, G. Zhao and W. F. Xie, First-principles study on electronic structure and optical properties of Sn-doped β-Ga$_2$O$_3$, *Physica B*, 2010, **405**, 3899–3903.

17 W. Z. Xiao, L. L. Wang, L. Xu, Q. Wan and A. L. Pan, Electronic structure and magnetic properties in nitrogen-doped-Ga$_2$O$_3$ from density functional calculations, *Solid State Commun.*, 2010, **150**, 852–856.

18 A. Kumar and U. Singisetti, First principles study of thermoelectric properties of β-gallium oxide, *Appl. Phys. Lett.*, 2020, **117**, 262104.

19 Y. J. Zhang, J. L. Yan, Q. S. Li, C. Qu, L. Y. Zhang and T. Li, Structural and optical properties of N-doped β-Ga$_2$O$_3$ films deposited by RF magnetron sputtering, *Physica B*, 2011, **406**, 3079–3082.

7048 | *Phys. Chem. Chem. Phys.*, 2022, **24**, 7045–7049

This journal is © the Owner Societies 2022

20 Y. J. Zhang, J. L. Yan, Q. S. Li, C. Qu, L. Y. Zhang and W. F. Xie, Optical and structural properties of Cu-doped β-Ga$_2$O$_3$ films, *Mater. Sci. Eng., B*, 2011, **176**, 846–849.

21 L. Y. Zhang, J. L. Yan, Y. J. Zhang, T. Li and X. W. Ding, First-principles study on electronic structure and optical properties of N-doped p-type β-Ga$_2$O$_3$, *Sci. China: Phys., Mech. Astron.*, 2012, **55**, 19–24.

22 S. Seacat, J. L. Lyons and H. Peelaers, Orthorhombic alloys of Ga$_2$O$_3$ and Al$_2$O$_3$, *Appl. Phys. Lett.*, 2020, **116**, 232102.

23 W. S. Li, D. Saraswat, Y. Y. Long, K. Nomoto, D. Jena and H. G. Xing, Near-ideal reverse leakage current and practical maximum electric field in β-Ga$_2$O$_3$ Schottky barrier diodes, *Appl. Phys. Lett.*, 2020, **116**, 192101.

24 J. B. Varley, A. Perron, V. Lordi, D. Wickramaratne and J. L. Lyons, Prospects for n-type doping of (Al$_x$Ga$_{1−x}$)$_2$O$_3$ alloys, *Appl. Phys. Lett.*, 2020, **116**, 172104.

25 Z. A. Jian, S. Mohanty and E. Ahmadi, Deep UV-assisted capacitance-voltage characterization of post-deposition annealed Al$_2$O$_3$/β-Ga$_2$O$_3$ (001) MOSCAPs, *Appl. Phys. Lett.*, 2020, **116**, 242105.

26 S. J. Clark, M. D. Segall, C. J. Pickard, P. J. Hasnip, M. J. Probert, K. Refson and M. C. Payne, First principles methods using CASTEP, *Z. Kristallogr.*, 2005, **220**, 567–570.

27 D. Vanderbilt, Soft self-consistent pseudopotentials in a generalized eigenvalue formalism, *Phys. Rev. B: Condens. Matter Mater. Phys.*, 1990, **41**, 7892–7895.

28 S. Baroni, S. D. Gironcoli, A. D. Corso and P. Giannozzi, Phonons and related crystal properties from density-functional perturbation theory, *Rev. Mod. Phys.*, 2001, **73**, 515–562.

29 M. Marezio and J. P. Remeika, Bond lengths in the α-Ga$_2$O$_3$ structure and the high-pressure phase of Ga$_{2−x}$Fe$_x$O$_3$, *J. Chem. Phys.*, 1967, **46**, 1862–1865.

30 S. Geller, Crystal structure of β-Ga$_2$O$_3$, *J. Chem. Phys.*, 1960, **33**, 676–684.

31 H. H. Tippins, Optical absorption and photoconductivity in the band edge of β-Ga$_2$O$_3$, *Phys. Rev.*, 1965, **140**, A316–A319.

32 F. Tran and P. Blaha, Accurate band gaps of semiconductors and insulators with a semilocal exchange-correlation potential, *Phys. Rev. Lett.*, 2009, **102**, 226401.

33 M. Orita, H. Hiramatsu, H. Ohta, M. Hirano and H. Hosono, Preparation of highly conductive, deep ultraviolet transparent β-Ga$_2$O$_3$ thin film at low deposition temperatures, *Thin Solid Films*, 2002, **411**, 134–139.

34 Y. Oshima, E. G. Víllora, Y. Matsushita, S. Yamamoto and K. Shimamura, Epitaxial growth of phase-pure ε-Ga$_2$O$_3$ by halide vapor phase epitaxy, *J. Appl. Phys.*, 2015, **118**, 085301.

35 F. Boschi, M. Bosi, T. Berzina, E. Buffagni, C. Ferrari and R. Fornari, Hetero-epitaxy of β-Ga$_2$O$_3$ layers by MOCVD and ALD, *J. Cryst. Growth*, 2016, **443**, 25–30.

This journal is © the Owner Societies 2022

Phys. Chem. Chem. Phys., 2022, **24**, 7045–7049 | 7049